10TH INTERNATIONAL CONFERENCE ON SUSTAINABLE ENERGY AND ENVIRONMENTAL PROTECTION (JUNE 27TH – 30TH, 2017, BLED, SLOVENIA), RENEWABLE ENERGY SOURCES
J. Krope, A.Ghani Olabi, D. Goričanec & S. Božičnik

# Comparison of the Shading Influence on PV Modules of Different Technologies

GORAN KNEŽEVIĆ, DANIJEL TOPIĆ, MATEJ ŽNIDAREC, BOJAN ŠTUMBERGER, MIRALEM HADŽISELIMOVIĆ & SEBASTIJAN SEME

**Abstract** The characteristics of different PV modules are provided in this paper. The influence of shading on PV module characteristics of different technologies (different crystalline silicon and thin film technologies) is investigated. The study also took into account the orientation of PV modules (portrait or landscape), a by-pass diode number and a type of connections. An inter-row shading factor for different PV modules has also been determined. A comparison of shading influence on PV module characteristics of different technologies has been drawn. A shading factor comparison of different technology PV modules has also been made. The influence of shading on PV system electricity production has been modelled based on a study which examined the influence of shading on characteristics of different technology PV modules.

**Keywords:** • shading • influence • shading factor • PV modules technologies • comparison •

CORRESPONDENCE ADDRESS: Goran Knežević, Ph.D., Assistant Professor, J.J. Strossmayer University of Osijek, Faculty of Electrical Engineering, Computer Science and Information Technology Osijek, K. Trpimira 2B, 31000 Osijek, Croatia, e-mail: goran.knezevic@etfos.hr. Danijel Topić, Ph.D., Assistant Professor, J.J. Strossmayer University of Osijek, Faculty of Electrical Engineering, Computer Science and Information Technology Osijek, K. Trpimira 2B, 31000 Osijek, Croatia, e-mail: danijel.topic@etfos.hr. Matej Žnidarec, Assistant, J.J. Strossmayer University of Osijek, Faculty of Electrical Engineering, Computer Science and Information Technology Osijek, K. Trpimira 2B, 31000 Osijek, Croatia, e-mail: matej.znidarec@etfos.hr. Bojan Štumberger, Ph.D., Full Professor, University of Maribor, Faculty of Energy Technology, Hočevarjev trg 1, 8270 Krško, Slovenia, e-mail: bojan.stumberger@uni-mb.si. Miralem Hadžiselimović, Ph.D., Associate Professor, University of Maribor, Faculty of Energy Technology, Hočevarjev trg 1, 8270 Krško, Slovenia, e-mail: miralem.h@uni-mb.si. Sebastijan Seme, Ph.D., Associate Professor, University of Maribor, Faculty of Energy Technology, Hočevarjev trg 1, 8270 Krško, Slovenia, e-mail: sebasijan.seme@um.si.

https://doi.org/10.18690/978-961-286-061-5.19 ISBN 978-961-286-061-5

Available at: http://press.um.si.

## 1 Introduction

World's power generation is still mostly on fossil fuels based. Due to the problems of limited reserves of fossil fuels and climate changes in previous years, usage of renewable sources had significantly increased. In order to reduce $CO_2$ emissions and increase share of renewables many international agreements were signed (Kyoto, 1997 and 2005; Cancun, 2010; Lima, 2014; Paris 2015). On October 2014, EU adopted 2030 Climate and Energy Policy Framework with following conclusions [1]:

- At least 40 % domestic reduction in greenhouse gas emissions by 2030 compared to 1990.
- At least 27 % is set for the share of renewable energy consumed in the EU in 2030.
- At least 27 % is set for improving energy efficiency in 2030 compared to projections of future energy consumption.

According to [2], photovoltaics (PV) is a key technology option for implementing the shift to a decarbonised energy supply and can be deployed in a modular way almost everywhere on this planet and solar resources in Europe and across the world are abundant and cannot be monopolised by one country. PV is one of the fastest growing capacity in recent years. According to [2] PV capacity in 2014 was 177 GW and in the end of 2015 was 227 GW. That is nearly 10 times the world's cumulative PV capacity of a decade earlier [3]. Most of PV modules used in PV capacity are crystalline (mono or multi) modules. Production capacity of PV modules in 2015 was estimated in range of 63 GW to 69 GW. According to [3], production of the thin film PV modules in 2015 increased by an estimated 13%, accounting for 8% of total global PV production (down from 10% in 2014).

Many different factors influence on electricity generation of the PV modules. One of the factors that significantly influences on output power of the PV module is shading. Many researches about influence of shading are already conducted. In [4], shading effects on current – voltage characteristic of a mono-crystalline PV module is investigated. Experimental model for estimation of energy losses in PV arrays caused by shading is presented in [5]. In [6], influence of partial shading on of characteristics of the PV modules with different connection configuration of cells is investigated. Electrical characteristics and operation of series connected modules in condition of partial shading using MATLAB model is investigated in [7]. Shading factor which depends on the ratio of sunny part of the module and total module area is introduced by [8]. Discrete current-voltage model for partially shaded PV arrays using Newton-Raphson algorithm, interpolation methods and analytical approximations is presented in [9]. In [10], influence of shading on CIGS PV modules is presented. Effects of shading on PV systems are also investigated in [11], [12], [13] and [14].

Aim of this paper is to investigate influence of shading on characteristics of different PV modules technologies and drawn comparison. Following PV module technologies are investigated: mono-crystalline, multi crystalline, high-efficient monocrystalline, a-Si thin film and CIS thin film. Based on measurements results, the influence of shading on PV system electricity production has been modelled.

## 2 Methodology

In this chapter proposed methodology will be described. Methodology consists: measurement procedure, calculation of shading factor and description of the used mathematical model.

### 2.1 Measurement procedure

Measurements of influence of the shading on the characteristics of PV modules of different technologies is conducted. Following PV modules technologies were tested: mono-crystalline, multi crystalline, high-efficient monocrystalline, a-Si thin film and CIS thin film. Measurements were conducted in ResLAB. In Figure 1, measurement procedure is presented.

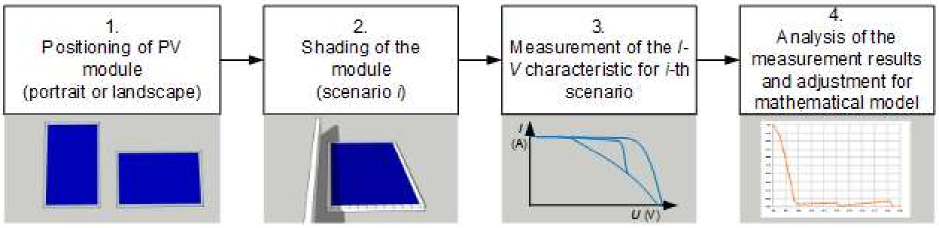


Figure 1. Measurement Procedure

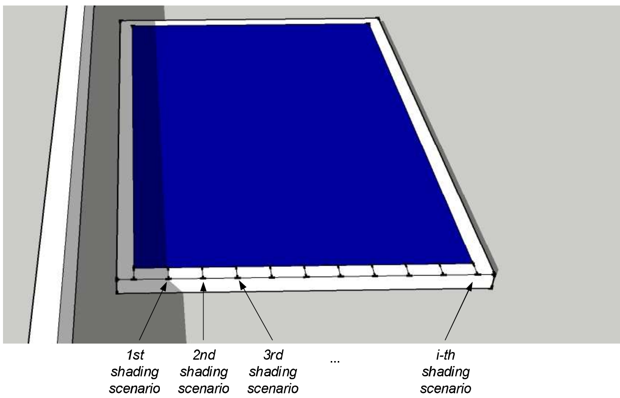


Figure 2. Shading Scenarios

Influence of shading on characteristics of PV modules for landscape and portrait orientations of PV modules is investigated. Shading of the module scenarios are presented in figure 2. First scenario is: 8 % of the module area in landscape orientation is shaded, second scenario: 16 % of the module area in landscape orientation is shaded, etc. Then same procedure is applied for portrait orientation with step of 5 % of area. Same shading scenarios for all five PV module technologies are repeated.

### 2.2 Calculation of the shading factor

As presented in [8], the influence of shading on PV module output power can be taken into account by shading factor $\eta_s$ depending on the ratio of the sunny part of the module $A_s$ and the total module surface $A$ as in (1):

$$\eta_s = \frac{P_s}{\frac{A_s}{A} \times P_t} \tag{1}$$

where $P_s$ is the measured output power of the partially shaded module and $P_t$ is the output power of the unshaded module. In this way, calculated shading factor can be represented as a function of the ratio $A_s/A$. In addition, piecewise linear approximation of obtained function $\eta_s(A_s/A)$ can be performed so the shading factor then can be easily calculated according to the given ratio of the sunny part and the total module surface.

### 2.3 Description of the used mathematical model

Expression for calculating an annual energy production of PV system for the given installation area taking into account the influence of the inter-row shading on the PV module output power is presented in (2) [8].

$$W_{\beta,r} = \sum_{i}^{365}\sum_{j}^{np}\frac{0,25}{1000}G_{\beta,i,j}A\cdot\eta_r\cdot n_{\theta_{\beta,i,j}}\cdot n_{d_\beta}\cdot\left(1+(r-1)\cdot\frac{1+\frac{d}{b\cdot\cos\beta}}{1+\frac{\tan\beta}{\mathrm{tg}\alpha_{i,j}}}\cdot\eta_s\right)[\mathrm{kWh}] \tag{2}$$

Where:

| | |
|---|---|
| $np$ | - the number of 15-minute periods in one day |
| $G_{\beta,i,j}$ | - average insolation in a 15-minute period $j$ in a day $I$ for the given module angle β; |
| $A$ | - size of a total PV module surface in one row; |
| $\eta_r$ | - rated efficiency of the observed PV module; |
| $n_{\theta_{\beta,i,j}}$ | - temperature factor in a 15-minute period $j$ in a day $i$ for the given module angle $\beta$; |
| $n_{d_\beta}$ | - dust factor for the given module angle $\beta$; |
| $r$ | - number of rows in the solar power plant; |

$d$ - distance between PV module rows;
$b$ - PV module width;
$a$ - PV module length;
$\beta$ - PV module angle;
$\alpha_{i,j}$ - the angle of the sun for period $j$ in a day $i$.
$\eta_s$ - shading factor.

The distance between module rows can be calculated as in (3) [8].

$$d = \frac{ap - b \cdot r \cdot \cos\beta}{r-1} \quad (3)$$

Where:

$ap$ - width of the parcel (across the module rows);
$bp$ - length of the parcel (along the module rows);
$nmr$ - number of modules in one row.

The number of modules in one row and the size of the total module surface in one row can be calculated as:

$$nmr = floor\left(\frac{bp}{a}\right) \quad (4)$$

$$A = nmr \cdot a \cdot b \quad (5)$$

The correlation between the ratio of the sunny and the total part of the module surface of the row following the first row, angle of the sun, angle of the PV module, distance between module rows and module equals [8]:

$$\frac{As}{A} = \frac{1 + \frac{d}{b \cdot \cos\beta}}{1 + \frac{\tan\beta}{\mathrm{tg}\alpha}} \quad (6)$$

In order to maximize the annual energy production on the observed installation area, the optimal number of rows and a module angle can be determined by calculating the annual production for the given range of $r$ and $\beta$ and finding the maximal value of the production whose indexes show the optimal $r$ and $\beta$.

The model is created in MATLAB. In a double *for loop* for the given range of $r$ and $\beta$, $W_{\beta,r}$ is calculated for each pair of $r$ and $\beta$ using expression (2) and taking into account expressions (3)-(5). The obtained matrix of annual energy production related to tested $r$

and $\beta$ is then searched for the maximal value which then reveals the optimal value of $r$ and $\beta$.

## 3 Case Study

### 3.1 Case scenario description

Optimal configuration of PV systems providing maximal annual energy production for different module types and different module orientation are determined for available installation area in Osijek, Croatia, oriented as it is shown in Fig. 3.

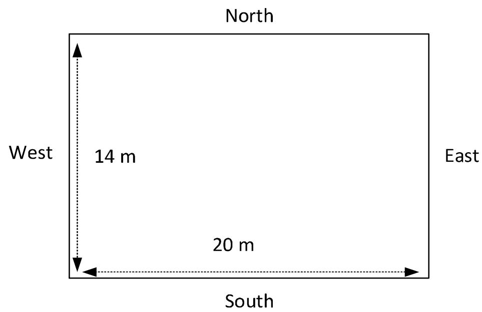


Figure 3. Orientation of Observed Area of the Installation of the PV Modules

For the given latitude (45°33′24″N) and longitude (18°41′44″E), the average daily solar irradiance $G$ for a 15-minute periods on a fixed plane are taken from PVGIS [15] for the south orientation and inclination β in the step of 1 degree for a range of 5 to 40 degrees. Cases with module angle less than 5 degrees are not considered due to significant influence of dust deposition [16], [17] and [18]. Technical characteristics of PV modules on which measurements were conducted are given in Table 1

Table 2. Technical characteristics of the tested PV modules [19], [20],[21],[22] and [23]

| | Bisol BMO 250 | Bisol BMU 250 | Panasonic VBHN240 | Solar Frontier SF-150 | Masdar MPV100-S |
|---|---|---|---|---|---|
| Maximum Power (W) | 250 | 250 | 240 | 150 | 100 |
| Short Circuit Current (A) | 8.8 | 8.75 | 5.85 | 2.2 | 1.57 |
| Open Circuit Voltage (V) | 37.9 | 38.4 | 52.4 | 108 | 100 |
| MPP Current (A) | 8.2 | 8.25 | 5.51 | 1.85 | 1.33 |
| MPP Voltage (V) | 30.5 | 30.3 | 43.7 | 81.5 | 76 |
| Power Temperature Coefficient $\gamma$ (%/°C) | -0.39 | -0.35 | -0.3 | -0.31 | -0.2 |
| NOCT (%) | 44 | 44 | 48.3 | 47 | N/A |
| Module Efficiency (%) | 15.3 | 15.3 | 19 | 12.2 | 6.99 |
| Module Efficiency under Real-Life Conditions* (%) | 14.15 | 14.15 | N/A | 9.04 | N/A |
| Length (mm) x Width (mm) x Thickness (mm) | 1649 x 991 x 40 | 1649 x 991 x 40 | 1580 x 798 x 35 | 1257 x 977 x 35 | 1300 x 1100 x 32 |

### 3.2 Measurement results

In order to determine the influence of shading on the output power of each tested PV module, the measurement is conducted in the Laboratory for sources of Faculty of Electrical Engineering, Computer Science and Information Technology Osijek. Measurement is performed as it is described in Chapter 2.1.

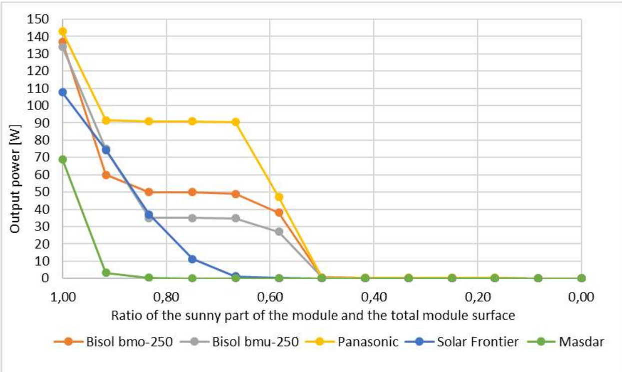


Figure 4. Measurement Results of the Output Power of the Landscape Oriented PV Modules in Respect to *As/A*

Measurement results of the output power of the landscape oriented PV modules in respect to the ratio of the sunny part and the total module surface are presented in Figure 4.
The shading factor is calculated for each measurement step using expression (1). Calculated values of the shading factor of the landscape oriented PV modules in respect to the ratio of the sunny part and the total surface is presented in figure 5.

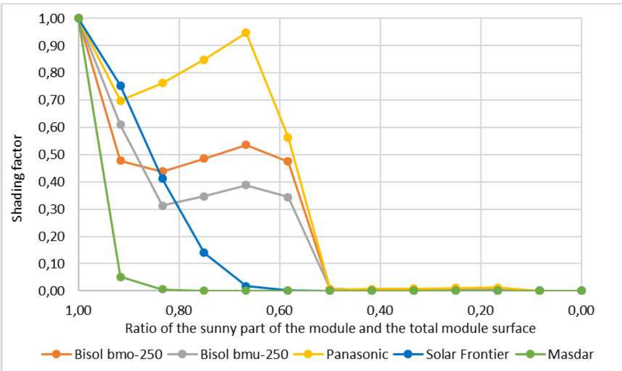


Figure 5. Calculated values of the shading factor of the landscape oriented PV modules in respect to *As/A*

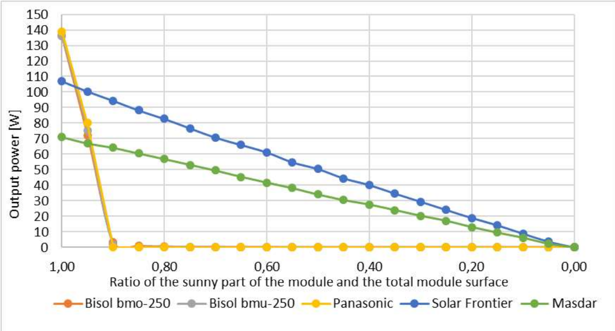


Figure 6. Measurement Results of the Output Power of the Portrait Oriented PV Modules in Respect to *As/A*

Piecewise linear approximation is conducted and the function $\eta_s(A_s/A)$ is obtained. Thus, when calculating energy production using (2), a shading factor is calculated according to the given ratio of the sunny part and the total module surface that can be calculated using (6). Measurement results of the output power of the portrait oriented PV modules in respect to the ratio of the sunny part and the total module surface are presented in Figure 6.

Calculated values of the shading factor of the portrait oriented PV modules in respect to the ratio of the sunny part and the total module surface are presented in Figure 7. Piecewise linear approximation is conducted and the function $\eta_s(A_s/A)$ is obtained.

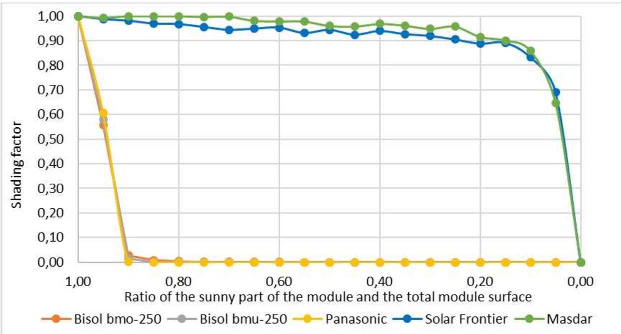


Figure 7. Calculated values of the shading factor of the portrait oriented PV modules in respect to *As/A*

### 3.3 Calculation of expected energy production for different PV modules

Optimal configuration of PV systems providing maximal annual energy production for different module types and different module orientation are determined as it is described in Chapter 2.3.

For example, annual energy production of BMU 250 PV module (landscape orientation) in respect to the number of rows for the given module angle is presented in Figure 8.

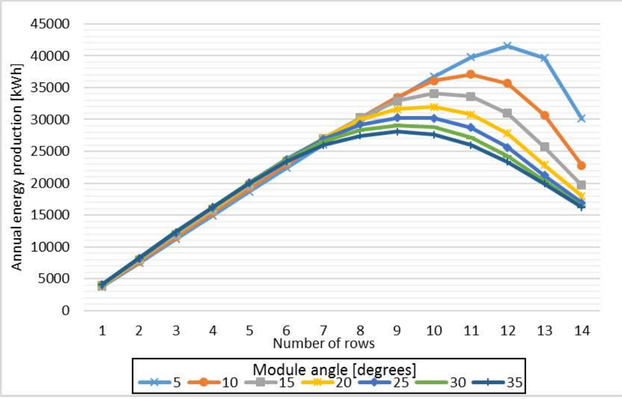


Figure 8. Annual energy production of BMU 250 PV module (landscape orientation) in respect to the number of rows

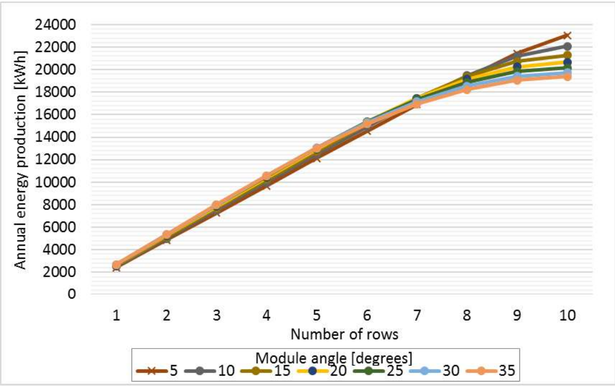


Figure 9 Annual energy production of Masdar PV module (portrait orientation) in respect to the number of rows

The annual energy production of Masdar PV module (portrait orientation) in respect to the number of rows for the given module angle is presented in Figure 9.

Table 2. Optimal configuration of PV power system providing maximal annual production for landscape (L) and portrait (P) orientation

| Module Type | Optimal number of rows | Optimal angle [degrees] | Number of modules in one row | Total number of modules | Maximum power [kWp] | Annual production [kWh] |
|---|---|---|---|---|---|---|
| Bisol BMO 250 | 12(L); 7(P) | 5(L); 5(P) | 12(L); 20(P) | 144(L); 140(P) | 36(L); 35(P) | 41395,7(L); 46782,2 (P) |
| Bisol BMU 250 | 12(L); 7(P) | 5(L); 5(P) | 12(L); 20(P) | 144(L); 140(P) | 36(L); 35(P) | 41550,4(L); 43927,0 (P) |
| Panasonic | 14(L); 7(P) | 5(L); 5(P) | 12(L); 25(P) | 168(L); 175(P) | 40,32(L); 42(P) | 52649,1(L); 53842,4 (P) |
| Solar Frontier | 12(L); 11(P) | 5(L); (P) | 15(L); 20(P) | 180(L); 220(P) | 27(L); 33(P) | 34209,1(L); 39675,3 (P) |
| Masdar | 10(L); 10(P) | 5(L); (P) | 15(L); 18(P) | 150(L); 180(P) | 15(L); 18(P) | 19096,1(L); 23059,0 (P) |

## 4 Conclusion

In this paper influence of shading on output power of different PV modules technologies in respect to shaded area is presented. Optimal configuration of the PV system with different PV module technologies providing maximal annual production for landscape and portrait orientation of the modules is determined.

### References

[1] European Commission, “2030 climate & energy framework | Climate Action,” *Ec.Europa.Eu*, 2016. [Online]. Available: https://ec.europa.eu/clima/policies/strategies/2030_en. [Accessed: 23-Mar-2017].

[2] W. E. Commission, P. V. S. Report, and F. E. Technologies, *PV Status Report 2016 PV Status Report 2016*, no. October. 2016.

[3] Kristin Seyboth *et al.*, *Renewables 2016 Global Status Report*. 2016.

[4] S. Seme, “XII International PhD Workshop Shading effects in the IU characteristic of a mono-crystalline PV module,” no. October, pp. 23–26, 2010.

[5] F. Martínez-Moreno, J. Muñoz, and E. Lorenzo, “Experimental model to estimate shading losses on PV arrays,” *Sol. Energy Mater. Sol. Cells*, vol. 94, no. 12, pp. 2298–2303, 2010.

[6] Y. J. Wang and P. C. Hsu, “An investigation on partial shading of PV modules with different connection configurations of PV cells,” *Energy*, vol. 36, no. 5, pp. 3069–3078, 2011.

[7] A. Mäki, S. Valkealahti, and J. Leppäaho, “Operation of series-connected silicon-based photovoltaic modules under partial shading conditions,” *Prog. Photovoltaics Res. Appl.*, 2012.

[8] D. Topić, G. Knežević, and K. Fekete, “The mathematical model for finding an optimal PV system configuration for the given installation area providing a maximal lifetime profit,” *Sol. Energy*, vol. 144, pp. 750–757, 2017.

[9] E. Díaz-Dorado, J. Cidrás, and C. Carrillo, “Discrete I-V model for partially shaded PV-arrays,” *Sol. Energy*, vol. 103, pp. 96–107, 2014.

[10] N. G. Dhere, E. Schneller, and A. Kaul, “Effect of shading on CIGS thin film photovoltaic modules,” *2015 IEEE 42nd Photovolt. Spec. Conf. PVSC 2015*, no. 321, pp. 0–2, 2015.

[11] M. A. Ghasemi, H. Mohammadian Forushani, and M. Parniani, “Partial shading detection

and smooth maximum power point tracking of PV arrays under PSC," *IEEE Trans. Power Electron.*, vol. 31, no. 9, pp. 6281–6292, 2016.
[12] L. Fialho, R. Melicioa, V. M. F. Mendes, J. Figueiredo, and M. Collares-Pereiraa, "Effect of Shading on Series Solar Modules: Simulation and Experimental Results," *Procedia Technol.*, vol. 17, pp. 295–302, 2014.
[13] S. Pareek and R. Dahiya, "Enhanced power generation of partial shaded photovoltaic fields by forecasting the interconnection of modules," *Energy*, vol. 95, pp. 561–572, 2016.
[14] M. Seyedmahmoudian, S. Mekhilef, R. Rahmani, R. Yusof, and E. T. Renani, "Analytical modeling of partially shaded photovoltaic systems," *Energies*, vol. 6, no. 1, pp. 128–144, 2013.
[15] "PV potential estimation utility." [Online]. Available: http://re.jrc.ec.europa.eu/pvgis/apps4/pvest.php#. [Accessed: 10-Apr-2017].
[16] A. Sayyah, M. N. Horenstein, and M. K. Mazumder, "Energy yield loss caused by dust deposition on photovoltaic panels," *Sol. Energy*, vol. 107, pp. 576–604, 2014.
[17] M. Mani and R. Pillai, "Impact of dust on solar photovoltaic (PV) performance: Research status, challenges and recommendations," *Renew. Sustain. Energy Rev.*, vol. 14, pp. 3124–3131, 2010.
[18] R. Appels *et al.*, "Effect of soiling on photovoltaic modules," *Sol. ENERGY*, vol. 96, pp. 283–291, 2013.
[19] Bisol, "Bisol BMO 250 datasheet," 2015. .
[20] Bisol, "Bisol BMU 250 datasheet," 2014. .
[21] S. Frontier, "Solar FrontierSF150-S." .
[22] Masdar, "Masdar MPV100-S datasheet," 2014. .
[23] Panasonic, "Panasonic VBHN240SE10 datasheet," 2012. .